NCOMMS-25-01529A
Final revised version

Graphene oxide increases the phototransduction efficiency of copolymeric nanoimplants and rescues visual functions in rat and pig models of *Retinitis pigmentosa*

F. Galluzzi[1,2]*, S. Francia[3]*, S. Cupini[1,4]*, T. Gianiorio[1,4], G. Mantero[1], M.L. DiFrancesco[3], T. Ravasenga[1,3], Jasnoor[1,4], M. Attanasio[5], J. F. Maya-Vetencourt[1,6], G. Pertile[5], D. Ventrella[7], A. Elmi[7], M.L. Bacci[7], S. Di Marco[1,3], F. Benfenati[1,4]*, E. Colombo[1,3]*

[1]Center for Synaptic Neuroscience and Technology, Istituto Italiano di Tecnologia, Genova, Italy; [2]The Open University Affiliated Research Centre at Istituto Italiano di Tecnologia (ARC@IIT); [3]IRCCS Ospedale Policlinico San Martino, Genova, Italy; [4]Department of Experimental Medicine, University of Genova, Italy; [5]Department of Ophthalmology, IRCCS Sacrocuore Don Calabria Hospital, Negrar, Verona, Italy; [6]Department of Biology, University of Pisa, Italy; [7]Department of Veterinary Medical Sciences, University of Bologna, Bologna, Italy.

* Equal contribution

Supplementary Information

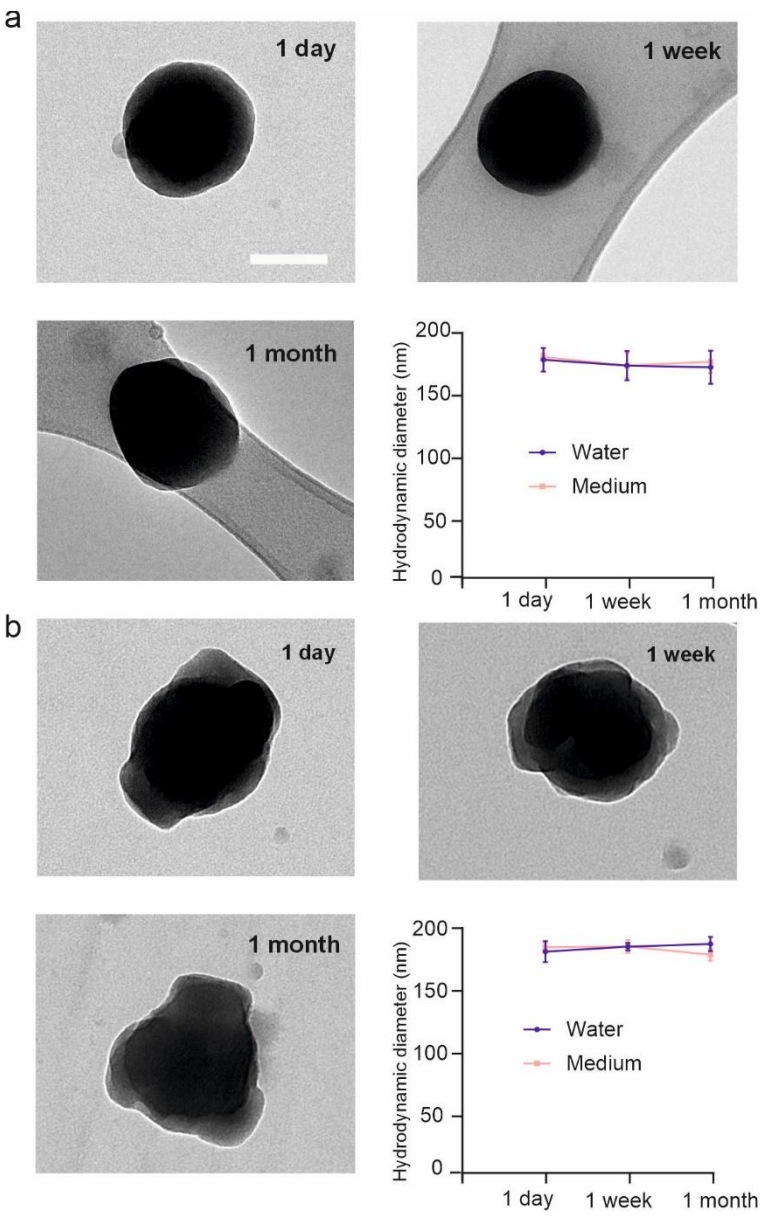

Supplementary Figure 1. The nanoimplants show colloidal stability in culture medium. Representative TEM images of PP **(a)** and PPG **(b)** nanoimplants acquired in Neurobasal medium after 1 day, 1 week, and 1 month, respectively, of incubation at 37 °C (scale bar, 100 nm). The hydrodynamic diameter of the PP **(a)** and PPG nanoimplants **(b)** acquired via DLS over time shows stability in both water and medium and no sign of aggregation (n = 3 independent batches).

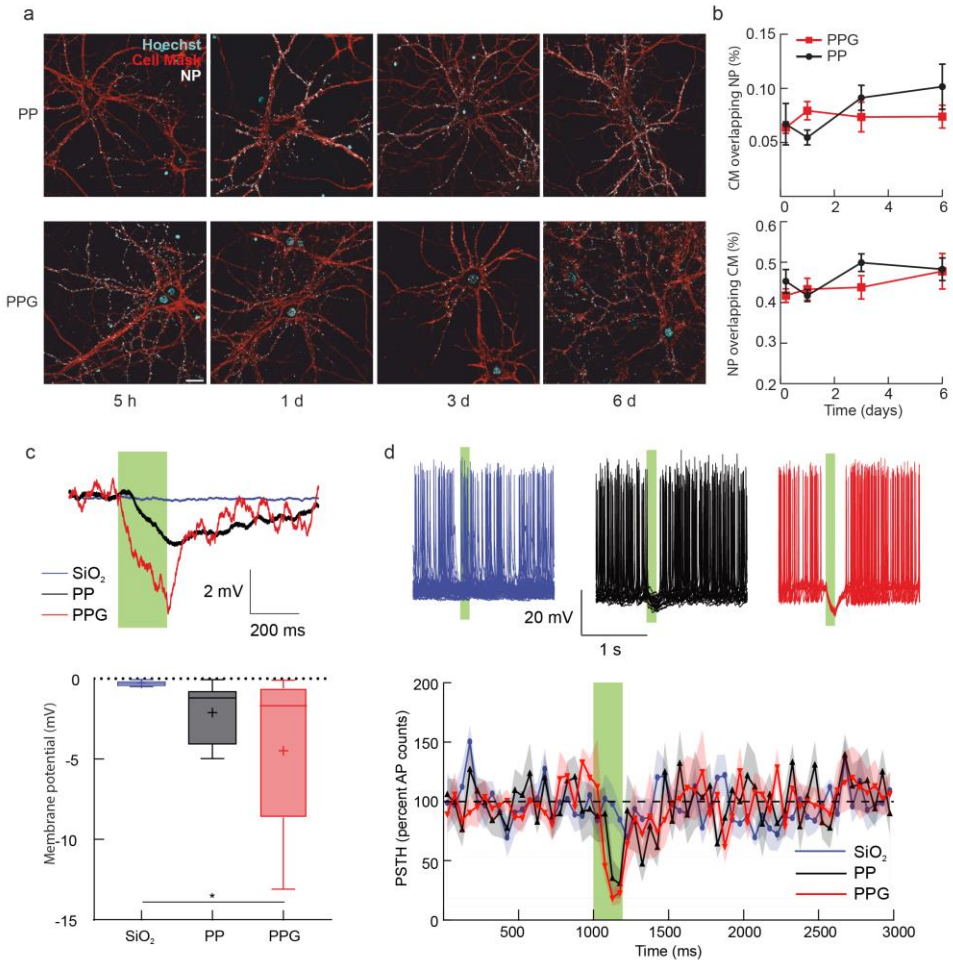

Supplementary Figure 2. Morphological and functional characterization of nanoimplants in primary neurons. (a) Representative live confocal images of primary hippocampal neurons incubated with either PPs (*top row*) or PPGs (*bottom row*) and observed over time from 5 h to 6 days (white). Cells were stained with Cell Mask (red) to label the cell plasma membrane and Hoechst (cyan) to label cell nuclei (scale bar, 20 µm). **(b)** Manders' coefficients analysis shows a similar extent of colocalization for both PPs and PPGs with Cell Mask-labeled plasma membranes (n=5 AF from at least 3 independent cultures), indicating similar affinities for the cell membrane. **(c)** Light-induced membrane voltage modulation was measured in a current-clamp configuration with no current injection (I=0). *Upper panel:* Representative traces of primary hippocampal neurons incubated with SiO_2 (blue), PPs (black), or PPGs (red) in response to light stimulation at 15 mW/mm^2 for 200 ms (green shaded area). *Lower panel:* Box plots of the light-induced membrane hyperpolarization for the three types of materials. **(d)** Light-dependent firing modulation was measured in a current-clamp configuration with no-current injection (I=0). *Upper panel:* Representative traces of action potentials from hippocampal neurons incubated with SiO_2 (blue), PPs (black), or PPGs (red) in response to light stimulation at 15 mW/mm^2 for 200 ms (green shaded area). *Lower panel:* Peristimulus Time Histogram (PSTH) analysis (bin size, 50 ms) of action potential firing normalized to the 1-s prepulse firing activity. The green-shaded area corresponds to the light stimulus. *p<0.05, one-way ANOVA/Tukey's tests (n=9, 11, and 11 neurons for SiO_2, PPs and PPGs, respectively).

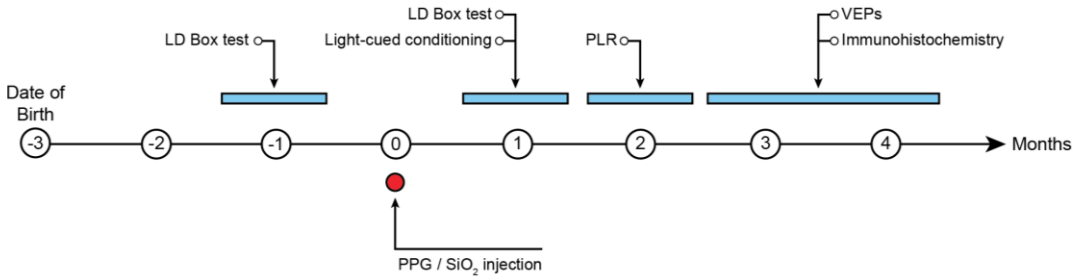

Supplementary Figure 3. Experimental timeline for functional testing of nanoimplants in the RCS rat. At 3-4 months of age, RCS rats underwent surgery for the subretinal injection of either inert SiO_2 or PPG particles. To test the effects of the nanoimplants on visual restoration, the light-driven behavior was investigated by the Light-Dark Box test 1 month before (MBI) and 1 month after injection (MPI). Light perception at the cortical level was studied using classical light-cued conditioning 1 MPI. *In vivo* physiological recordings were performed on the same animals, starting with the pupillary light reflex (PLR) at 2 MPI and subsequently recording visually evoked potentials (VEPs) at 3-4 MPI. After VEP recordings, animals were sacrificed, eyes were enucleated, and the dissected retina was subjected to the analysis of PPG distribution and immunohistochemistry.

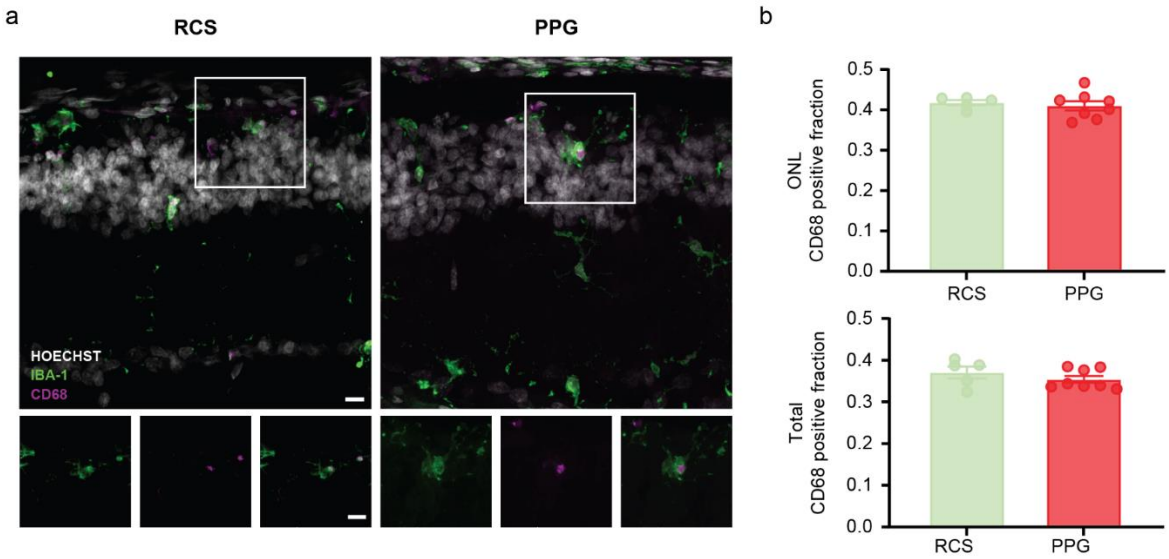

Supplementary Figure 4. Nanoimplant injection does not trigger microglia phagocytosis. **(a)** *Top:* Representative immunostaining of a non-injected RCS rat (*left*) and a PPG-injected RCS rat (*right*), labelled with Hoechst for cell nuclei (white), Iba1 for microglia (green), and CD68 for microglial activation (magenta). *Bottom:* 3× magnification showing individual Iba1 and CD68 channels, as well as their merged image (Scale bar, 10 µm). **(b)** Quantification of the fraction of CD68/Iba1-positive cells in the ONL (*top*) and in the entire retina (*bottom*) (n = 5, 8 animals for RCS and PPG, respectively). ONL, $p>0.5$; Total $p>0.3$; unpaired Student's *t*-test.

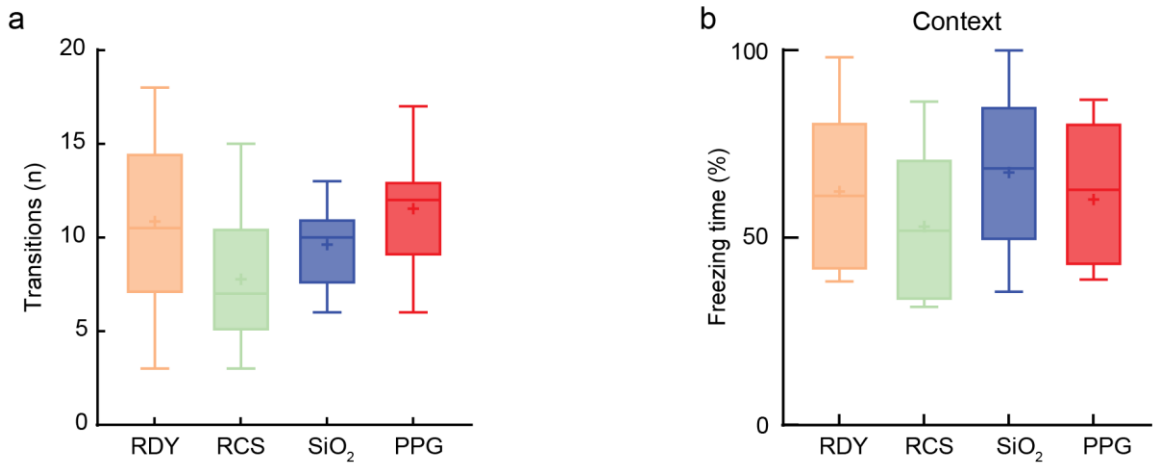

Supplementary Figure 5. Control tests in the behavioral evaluation of visual restoration in the RCS rat. (a) The number of transitions between the light and the dark compartments was monitored to rule out the possible presence of motor impairments interfering with the test results. No differences across the four experimental groups were observed (one-way ANOVA; RDY, n=14; RCS, n=9; SiO_2, n=8; PPG, n=11). **(b)** Freezing behavior in the context session was comparable among experimental groups, proving no environmental effects (one-way ANOVA; RDY, n=10; RCS, n=8; SiO_2, n=10; PPG, n=7).

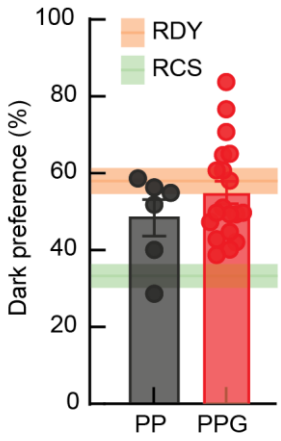

Supplementary Figure 6. Dark preference of PP- and PPG-injected RCS rats. The plot shows the comparison of the light/dark box performance of RCS rats that had been bilaterally injected with either PP (gray) or PPG (red) nanoimplants. Bars represent mean ± SEM with individual experimental points (n = 6 and 19 for RCS rats injected with PP and PPG, respectively). The orange and green horizontal lines and shaded areas represent the mean ± SEM of the control healthy RDY rats and dystrophic non-injected RCS rats (n = 21 and 17, respectively). PP *vs* RCS p=0.08; PPG *vs* RCS p<0.0001; Mann-Whitney's *U*-test.

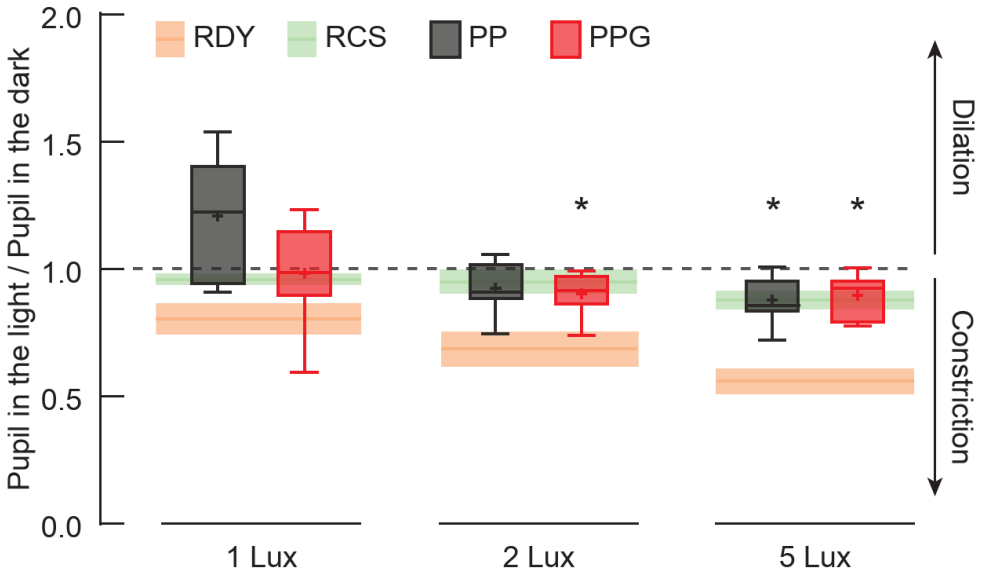

Supplementary Figure 7. PPG induces a stronger pupil constriction than PP at low luminance. Box plots of the extent of pupil constriction for a cohort of animals tested upon green light stimulation as a function of luminance (1, 2, and 5 Lux). The orange and green horizontal lines and shaded areas represent the means ± SEM of the pupillary responses observed in control healthy RDY rats (orange) and dystrophic non-injected RCS rats (green). PPG-injected RCS rats display a more marked pupillary constriction at low luminances with respect to non-injected or PP-injected animals. *$p<0.05$, one-sample Student's t-test against 1 (no constriction). RDY, n=6; RCS, n=8; PP, n=7, PPG, n=7.

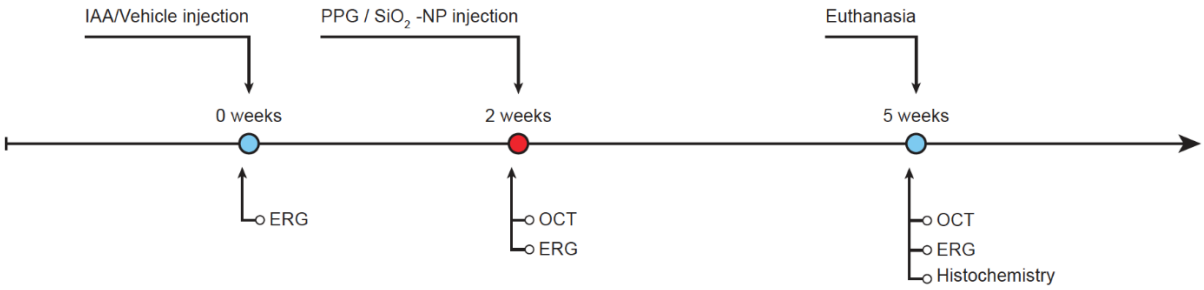

Supplementary Figure 8. Experimental timeline for IAA-lesion and functional testing of nanoimplants in the domestic pig. After baseline ERG recordings, 12-month-old domestic pigs, treated with either saline (vehicle) or IAA (12 mg/kg, intravenously), underwent the subretinal injection of either inert SiO_2 particles or PPGs two weeks later. *In vivo* ERG recordings were performed on the same animals 3 weeks after the PPG injection to test the effects on visual restoration. After ERG recordings, animals were sacrificed, eyes were enucleated, and the dissected retina was subjected to the histochemical analysis of PPG distribution and immunohistochemistry. The *in vivo* imaging of the retina was performed using OCT before and 3 weeks after the subretinal surgery.

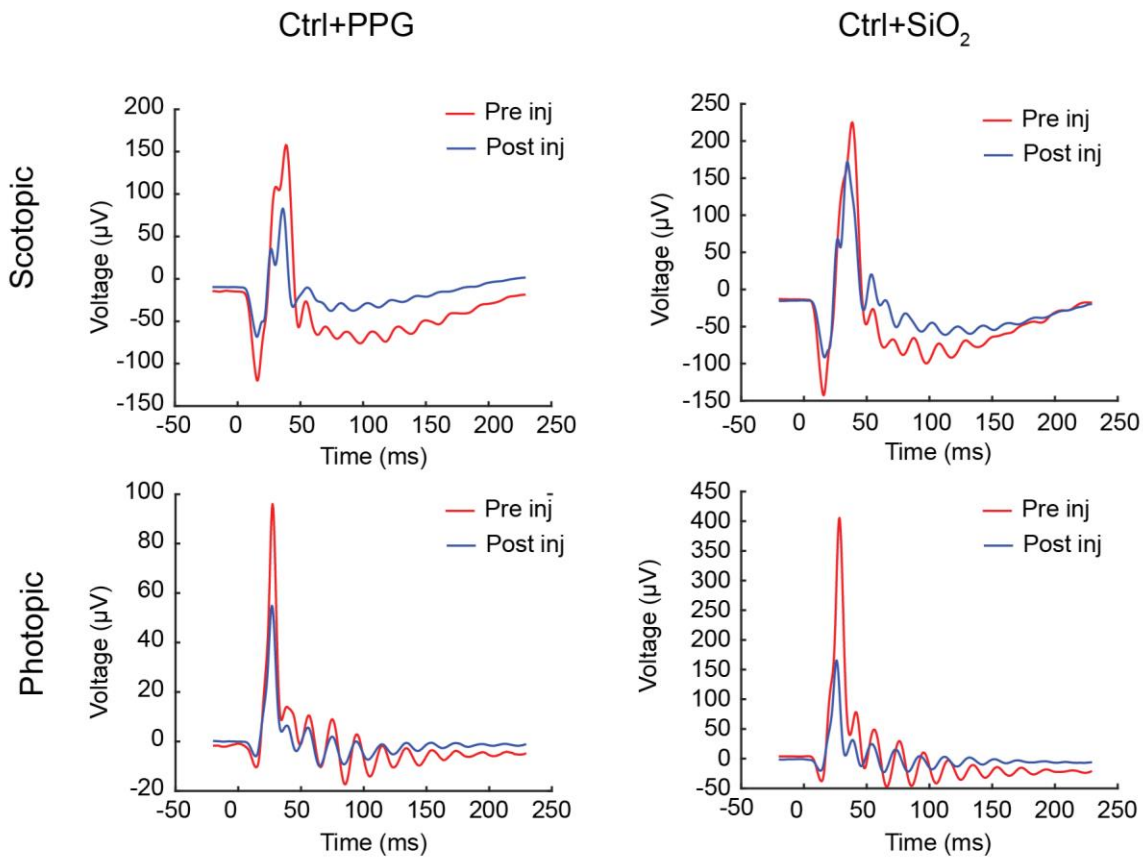

Supplementary Figure 9. ERG recordings in normal pigs after subretinal injection of nanoimplants. Representative ffERG traces for PPG- (*left*) and SiO_2- (*right*) injected healthy pigs under scotopic (*top*) and photopic (*bottom*) conditions before the surgery (red traces) and two weeks after surgery (blue traces). Both recordings showed a smaller amplitude for both the a-wave and b-wave two weeks after surgery.